

Influence of cooling speed on the physical and mechanical properties of granite in geothermal-related engineering

Longchuan Deng¹ | Xiaozhao Li^{1,2} | Yun Wu² | Fuqing Li² | Zhen Huang³ | Yukun Ji² | Chunjiang Zou⁴ | Zuxi Liu¹

¹School of Earth Sciences and Engineering, Nanjing University, Nanjing, Jiangsu, China

²State Key Laboratory for Geomechanics and Deep Underground Engineering, China University of Mining and Technology, Xuzhou, Jiangsu, China

³School of Resources and Environment Engineering, Jiangxi University of Science and Technology, Ganzhou, Jiangxi, China

⁴Department of Civil Engineering, Monash University, Melbourne, Australia

Correspondence

Xiaozhao Li, School of Earth Sciences and Engineering, Nanjing University, Nanjing 210046, Jiangsu, China.
Email: lixz@nju.edu.cn

Yun Wu, State Key Laboratory for Geomechanics and Deep Underground Engineering, China University of Mining and Technology, Xuzhou 221116, Jiangsu, China.
Email: wyl562254170@163.com

Funding information

The National Natural Science Foundation of China, Grant/Award Number: 41702326; the Innovative Experts, Long-term Program of Jiangxi Province, Grant/Award Number: jxsq2018106049; the Natural Science Foundation of Jiangxi Province, Grant/Award Number: 20202ACB214006; the Supported by Program of Qingjiang Excellent Young Talents, Jiangxi University of Science and Technology

Abstract

In deep-earth engineering, the high earth temperature can significantly affect the rock's mechanical properties, especially when the rock is cooled during the construction process. Accordingly, whether the cooling speed affects the mechanical and physical properties of rocks is worth to be investigated. The present study explored the influence of the cooling rate on the physical and chemical properties of granite heated at 25–800 °C. The mechanical and physical properties involved in this study included uniaxial compression strength, peak strain, modulus, P-wave velocity, mass and volume, the change of which could reflect the sensitivity of granite to the cooling rate. Acoustic emission (AE) monitoring, microscopic observation, and X-ray diffraction (XRD) are used to analyze the underlying damage mechanism. It is found that more AE signals and large-scale cracks are accounted for based on the b-value method when the specimens are cooled by water. Furthermore, the microscopic observation by polarized light microscopy indicates that the density, opening degree, and connectivity of the cracks under water cooling mode are higher than that under natural cooling mode. In addition, the XRD illustrates that there is no obvious change in mineral content and diffraction angle at different temperatures, which confirms that the change of mechanical properties is not related to the chemical properties. The present conclusion can provide a perspective to assess the damage caused by different cooling methods to hot rocks.

KEYWORDS

cooling methods, granite, high temperature, physical and mechanical properties, thermal damage

1 | INTRODUCTION

Heating treatment may create more cracks in the rock, and these thermally induced cracks would in turn change the rock's physical and mechanical properties (Ge & Sun, 2018; Murru et al., 2018; Nara et al., 2011; Souley et al., 2001; Z. W. Wang et al., 2021; X. G. Wu et al., 2018; Y. Wu et al., 2021). Moreover, once a high-temperature rock is put in cold media (water, nuclide), the number of cracks would increase, causing severe damage to the internal structure. Notably, this issue is related to different applications, including optimizing a

geothermal system and designing a highly radioactive waste disposal repository (Y. F. Chen et al., 2014). For example, when choosing a high-level radioactive waste disposal repository site, strict requirements would be placed upon the integrity of surrounding rocks. The surface temperature of the radioactive waste storage tanks can be as high as 300–500 °C, which exerts a thermal load on surrounding rocks and produces more cracks (Gens et al., 2002). If groundwater flows or there is a nuclide leak, the crack formations will be aggravated and further develop into a migration pathway for nuclide (Figure 1a) (S. Chen et al., 2017). Geothermal energy

This is an open access article under the terms of the Creative Commons Attribution License, which permits use, distribution and reproduction in any medium, provided the original work is properly cited.

© 2022 The Authors. *Deep Underground Science and Engineering* published by John Wiley & Sons Australia, Ltd on behalf of China University of Mining and Technology.

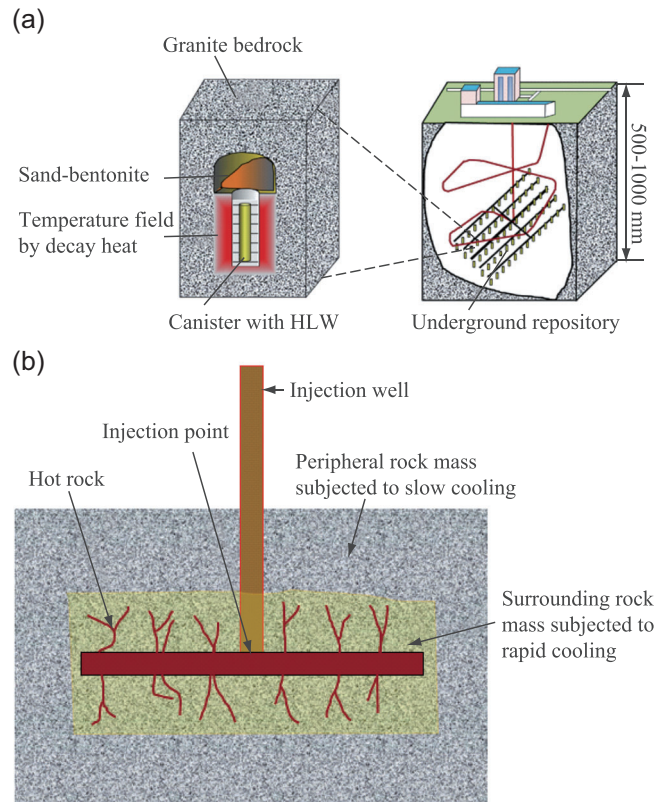


FIGURE 1 (a) Thermal problem in high-level radioactive waste repository (S. Chen et al., 2017); (b) Hot rock mass undergoes cooling during fluid injection (Avanthim & Gamage, 2018). HLW, high-level radioactive waste disposal.

extraction technology generates heat exchange between cold water and the hot dry rocks in deep underground. A cyclic heating load on surrounding rocks is produced, resulting in more cracks and changes in the physical and mechanical properties of rocks (Figure 1b) (Avanthim & Gamage, 2018). Therefore, it is important to study the formation of micro-cracks and the associated thermal damage of high-temperature rocks after rapid cooling. This can ensure the safety and durability of a radioactive waste disposal repository on the one hand and promote an effective geothermal system on the other.

Granite is widely used in constructing high radioactive waste disposal repositories and geothermal systems. The crack structure characteristics are a key geological factor to be considered in the design of the underground laboratory for disposing of highly radioactive waste. High temperature may change the physical and mechanical properties of granite and lead to crack propagation. As a result, the migration pathway of groundwater and nuclides would be affected. Once the temperature undergoes a drastic change, the tensile stress on the cooling surface of the granite and compressive stress inside granite is produced (Y. Chen & Wang, 1980). The number of thermally induced cracks increases with temperature, which leads to the increase in crack density and the changes of physical and mechanical properties of the rock (Cha et al., 2017; Xi et al., 2020). Great efforts have been made to explore the Theory of Thermal Damage in the context of brittle materials (e.g., rocks). As is revealed, the thermal damage degree is related to the heating mode, cooling mode, heating rate, and cooling rate (Shao et al., 2020; S. C. Wu et al., 2018; F. Zhang, Konietzky, et al., 2020; F. Zhang, Zhang, et al., 2020; W. Q. Zhang et al., 2016).

Most of the previous studies focused on the effect of heat and cooling methods on rocks. In fact, both cooling and heating treatments produce more cracks in the rock, resulting in decreasing elastic modulus and increasing permeability (Liu & Xu, 2015). However, the mechanism of heating and cooling treatment on the physical and mechanical properties of rocks is different. With the temperature rising, the property changes of rocks are caused under the effect of dewatering and mineral expansion. Meanwhile, with the temperature falling, the property changes of rocks are caused by internal thermal stress (W. Zhang et al., 2016). The thermal stress formed by rapid cooling weakens the bond force among rock mineral grains and changes the internal pore structure (Jin et al., 2019). C. Cai et al. (2014), C. Z. Cai et al. (2015), C. Z. Cai, Huang et al. (2016), and C. Z. Cai, Gao et al. (2016) conducted many experimental research, among which the most representative is a comparative study of the permeability and UCS in rapid cooling and slow cooling. As the results reveal, the number of cracks grows with the temperature rising. Other scholars and experts also carried out experimental and theoretical studies on heating and cooling modes (Han et al., 2020; Li et al., 2020; X. G. Wu et al., 2018), mainly from the macroscopic and microscopic perspectives. However, it is still difficult to combine macroscopic test results with microscopic features, such as establishing the relationship between rock strength and crack characteristics.

At present, the research methods of high-temperature rock mechanics mainly include rock mechanical tests, AE technology, infrared camera, scanning electron microscope (SEM), computed tomography (CT) technology,

nuclear magnetic resonance (NMR), XRD, and thin section analysis. Most of these focus on the investigation of cracks. For example, AE technology indirectly reflects the development of cracks during loading (Datt et al., 2015), while SEM and thin section analysis can observe the distribution characteristics of cracks inside the rock (Sun et al., 2017). Other studies analyzed the thermal damage mechanism from the perspective of mineral changes. W. Q. Zhang and Lv (2020) held that the mineral composition of limestone changed after heating. Although the abovementioned methods can effectively investigate the internal structure and mineral composition, some insightful views, such as the relationships between the crack characteristics and macro properties are worthy to be further investigated.

This paper mainly studies the changes in physical and mechanical properties, AE spatial and temporal evolution characteristics, crack distribution characteristics, and mineral changes of high-temperature granite after rapid cooling. The physical and mechanical characteristics of granite at 25–800 °C were analyzed, and the damage mechanism caused by heating and rapid cooling was revealed. The results obtained can provide insight into the establishment of the underground laboratory of the highly radioactive nuclear waste disposal repository and the optimization of geothermal energy extraction technology.

2 | EXPERIMENTAL SAMPLES AND METHODS

2.1 | Samples

The granite samples used in the experiment were collected from Shandong Province. In order to reduce the test error caused by specimen inhomogeneity, the test specimens were measured three times under the same condition. According to the requirements of

ISRM (Fairhurst & Hudson, 1999), the rocks were processed into cylinders of $\Phi 50 \times 100$ mm. As is shown in Figure 2, the surface color of the sample is bluish-white. The density and UCS of granite at room temperature were 2593 kg/m³ and 123 MPa, respectively. The main mineral compositions of Beishan granite are quartz, albite, microcline, and annite. A total of 48 granite samples were prepared to study the effects of cooling speed on the rock properties, and the samples were divided into 16 groups (8 for natural cooling and 8 for water cooling) with 3 samples in each group. They were heated from room temperature to 800 °C at a temperature interval of 100 °C.

2.2 | Methods and equipment

The experimental process and equipment in this study are shown in Figure 2. The granite samples were treated to the target temperature at a rate of 8 °C/min in a muff furnace. The samples were held at a constant temperature in the muffle furnace for 2 h after reaching the predetermined temperature (Figure 3). The water cooling was performed by immersing the whole specimen into the water to ensure the uniform thermal stress, while the natural cooling was performed in the muff furnace. According to the previous research results, the physical and mechanical properties of rocks that change correspondingly after heat treatment, mainly include mechanical strength, apparent color, P-wave velocity, permeability, porosity, and so on. To study the changes in physical and mechanical properties of granite after heat treatment under different cooling methods, a series of physical and mechanical indexes were tested, such as mass, apparent color, longitudinal wave velocity, UCS, AE characteristics, and microstructure. As is shown in Tables 1 and 2, the measured results were reliable at both natural and water cooling based on the mean

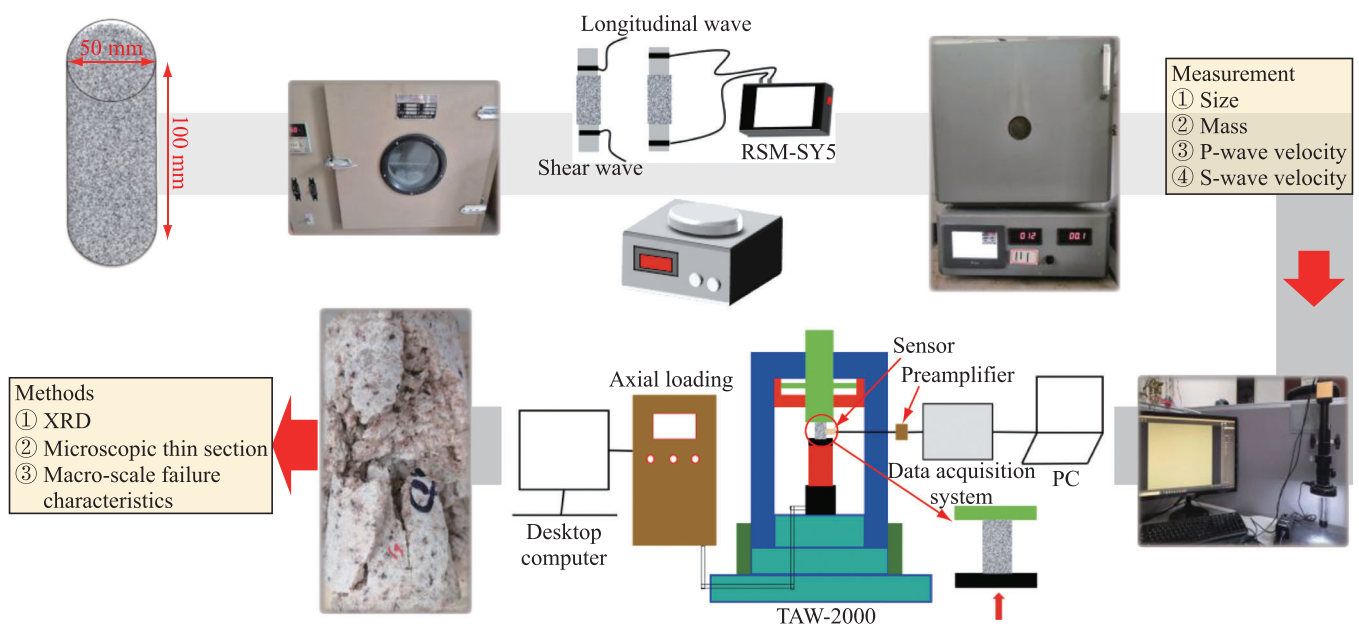


FIGURE 2 The experimental procedures and the test equipment

square deviation. The uniaxial compression test was carried out by the TAW-2000 rock triaxial testing machine; the loading mode was controlled by displacement at a rate of 0.1 mm/min. In the process of mechanical loading tests, AE was used for real-time monitoring. The AE monitoring device employed in the test was AMSY-6, produced and developed by the German Valley company. The parameters of acoustic emission equipment were set as follows: a threshold

value of 45 dB and an acquisition frequency of 5 MHz. An acoustic emission probe was placed in the center of the sample to reduce the influence of rock heterogeneity. Finally, the microstructure of the damaged samples was observed under a microscope.

3 | EXPERIMENT RESULTS AND ANALYSIS

3.1 | Microscopic observation of specimens

The apparent color of granite changes significantly after heating, as well as cooling modes (Table 3). The apparent color of granite is bluish-white originally and no obvious cracks can be observed at room temperature. After a high-temperature exposure shift from 25 °C to 400 °C, the granite gradually turned cyan color. However, light red appeared locally on the surface of granite when the high-temperature granite was cooled by water. When the experimental temperature was higher than 400 °C, the apparent color gradually developed to light red and the dark surface material became more prominent because the iron ions contained in the granite were oxidized to hematite.

The surface and internal structure of rocks are influenced by thermal stress (Chaki et al., 2008). The microscopy observation shows that no obvious cracks are formed when the heating temperature reaches 200–300 °C. Cracks can be

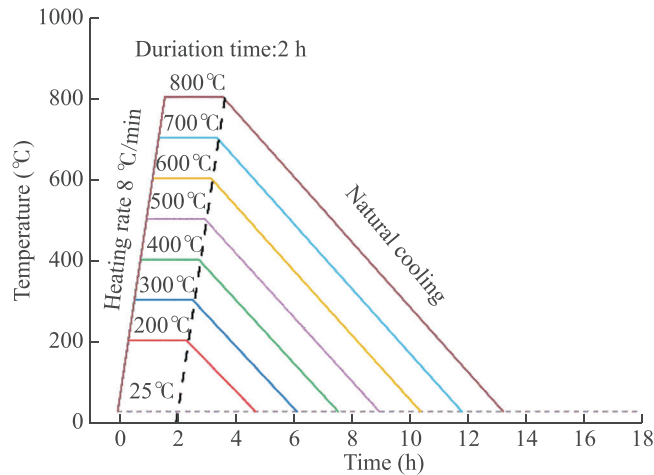


FIGURE 3 Schematic diagram of the heating path

TABLE 1 The mean square deviation for the measured results under natural cooling

Temperature (°C)	Peak stress (MPa)	Peak strain (%)	P-wave velocity (m/s)	S-wave velocity (m/s)	Volume expansion ratio (%)	Mass loss ratio (%)
25	2.3	0.03	37	34	0.000	0.000
200	1.5	0.01	46	54	0.011	0.009
300	1.7	0.05	23	26	0.009	0.012
400	4.1	0.04	16	71	0.012	0.021
500	3.9	0.03	43	39	0.008	0.017
600	2.5	0.05	27	50	0.123	0.062
700	2.4	0.01	42	64	0.131	0.132
800	4.1	0.02	87	29	0.098	0.105

TABLE 2 The mean square deviation for the measured results under water cooling

Temperature (°C)	Peak stress (MPa)	Peak strain (%)	P-wave velocity (m/s)	S-wave velocity (m/s)	Volume expansion ratio (%)	Mass loss ratio (%)
25	1.9	0.01	89	23	0.000	0.000
200	1.4	0.04	46	34	0.009	0.007
300	1.7	0.02	29	54	0.012	0.032
400	2.1	0.05	13	67	0.013	0.019
500	2.8	0.01	43	19	0.032	0.054
600	1.7	0.02	86	49	0.043	0.032
700	2.9	0.03	53	56	0.014	0.043
800	4.8	0.07	96	67	0.065	0.076

TABLE 3 Surface characteristics and microscopic picture of granite at different temperatures (the red lines and circles represent the cracks produced by thermal stress on the granite's surface)

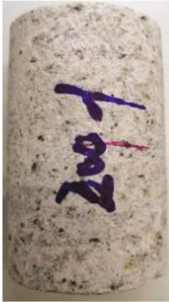

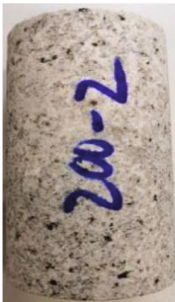
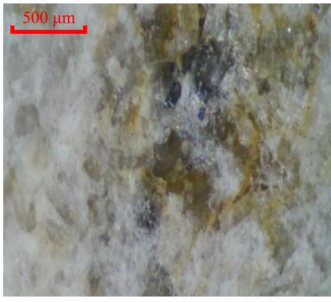
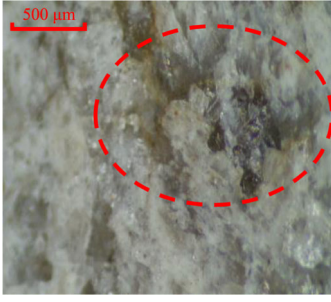
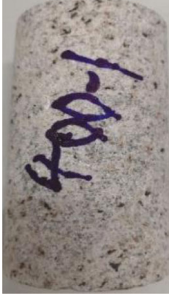
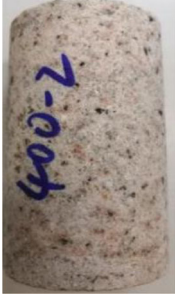








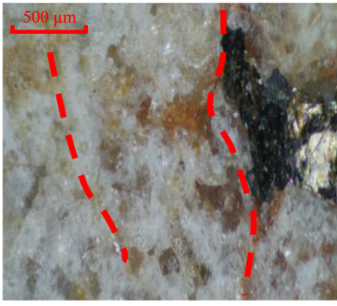

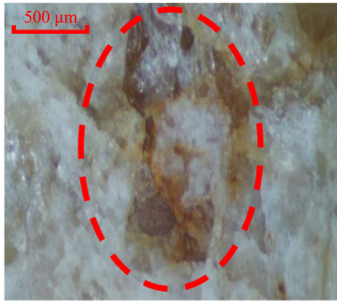

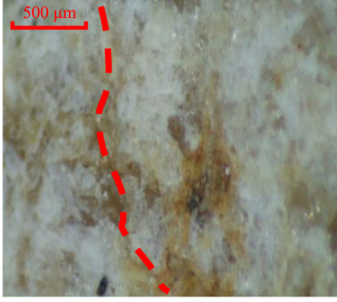

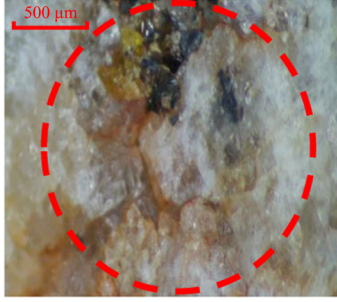
Temperature (°C)	Surface characteristics (Natural cooling)	Microscopic picture of surface (Natural cooling)	Surface characteristics (Water cooling)	Microscopic picture of surface (Water cooling)
200				
300				
400				
500				
600				

TABLE 3 (Continued)

Temperature (°C)	Surface characteristics (Natural cooling)	Microscopic picture of surface (Natural cooling)	Surface characteristics (Water cooling)	Microscopic picture of surface (Water cooling)
700				
800				

observed on the rock surface at 400 °C. With the further increase in temperature, there is also an increase in the number, size, and opening degree of surface cracks due to thermal stress, mineral phase change, and dehydration. Compared with the naturally cooled granite, the water-cooled granite has more cracks on the surface with larger opening degree. The mineral particles witness a large degree of uncoordinated deformation and the cracks are constantly expanding and penetrating due to the phase transition from α -quartz to β -quartz at 573 °C (Gomez-Heras et al., 2010). Additionally, partial particle shedding on the rock's surface and a greater opening degree of cracks occur due to thermal stress.

3.2 | Mechanical properties

The stress–strain response is useful for understanding the mechanical behavior of rocks. According to Avanthim and Gamage (2018) the initial nonlinear behavior of the stress–strain curve of brittle materials is caused by the compression of some pre-existing cracks under the axial force. Figure 4a shows that the nonlinear behavior region of the rock remains small when the temperature is below 500 °C; it expands gradually as the temperature rises above 500 °C. The brittleness of the granite also begins to lessen because the internal structure is weakened when the temperature exceeds 500 °C. This is specifically manifested as a shear failure with a diagonal crack or the crack distributed along the direction of maximum principal stress. Furthermore, the stress–strain response of granites between natural cooling and water cooling differs to some extent. To be specific, the failure strain under water cooling is generally greater than that under natural cooling; and the nonlinear region and toughness under water cooling are also generally greater than those under the natural cooling; This is mainly due to

the large number of micro-cracks formed under water cooling, which results in large deformations during loading. The results of this experiment are in line with those of Avanthim and Gamage (2018).

Temperature is an important factor affecting rock strength and deformation (Johnson et al., 1979; Liu & Xu, 2014; Urquhart & Bauer, 2015). Figure 5 shows the relationship between peak stress and temperature under different cooling modes. When the heating temperature rises from 25 °C to 400 °C, the peak stress increases slightly under natural cooling from 124 MPa at 25 °C to 135 MPa at 400 °C, with an increase of 8.9%. Concerning water cooling, the peak stress of granite decreases continuously with temperature, from 124 MPa at 25 °C to 92 MPa at 400 °C, with a decrease of 25.8%. Micro-cracks are produced by thermal stress at 25–400 °C; however, some of the original cracks close to some extent, which can improve the mechanical properties of the rock in small increments. It is also the main reason for the rise in peak stress under natural cooling (Wang et al., 2013). However, when the granite is cooled by the water, the internal stress exceeds the strength among mineral particles. As a result, more cracks would be formed, leading to the decrease in peak stress. With the further increase in temperature, the peak stress decreases under both cooling modes. Further, both heating and cooling cause visible damage to the rock when the temperature exceeds 400 °C. Vazquez et al. (2018) found that the cracks inside the granite would produce obvious damage when the temperature exceeded 400 °C, which was further proved by SEM. At the same time, quartz will undergo a phase transition at 573 °C, which consequentially changes its mechanical properties. As is indicated by the test results, the peak stress of the granite when it is cooled by water is lower than that when it is cooled naturally.

Figure 6 shows the variation of peak strain with temperature under two cooling modes. In a word, the

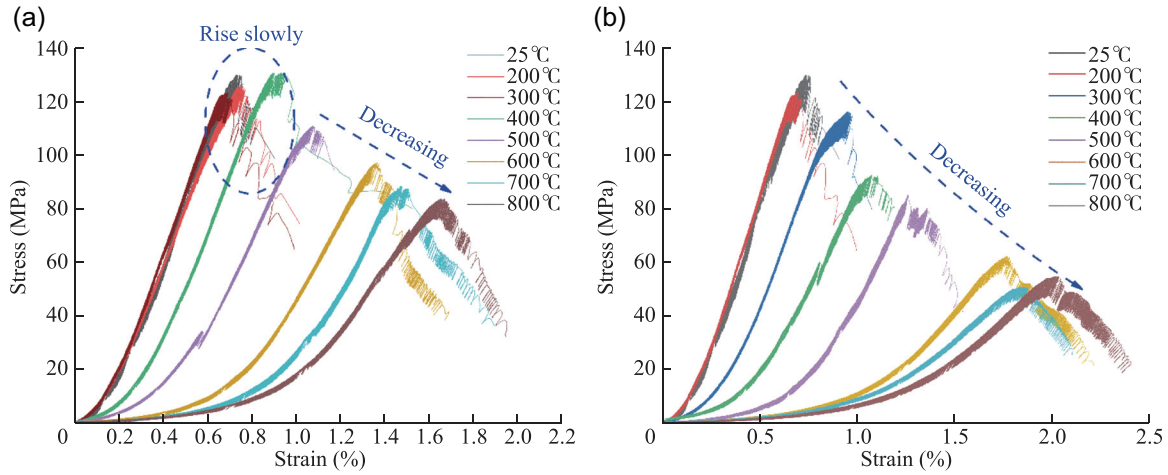


FIGURE 4 Characteristics of stress–strain at different temperatures under different cooling modes: (a) Natural cooling; (b) Water cooling

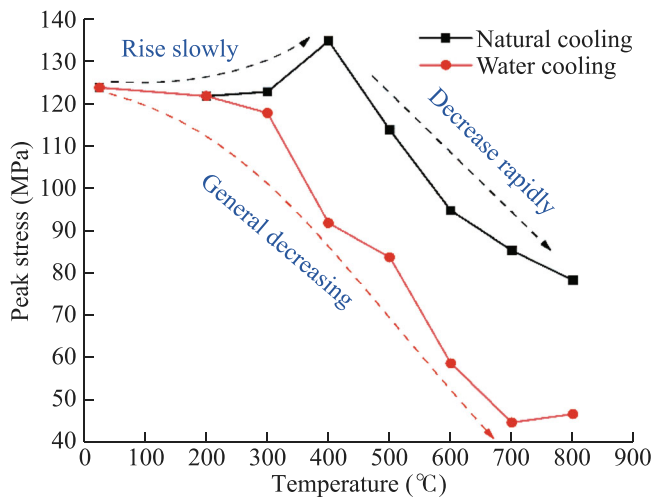


FIGURE 5 Variation of peak stress with the temperature under different cooling modes

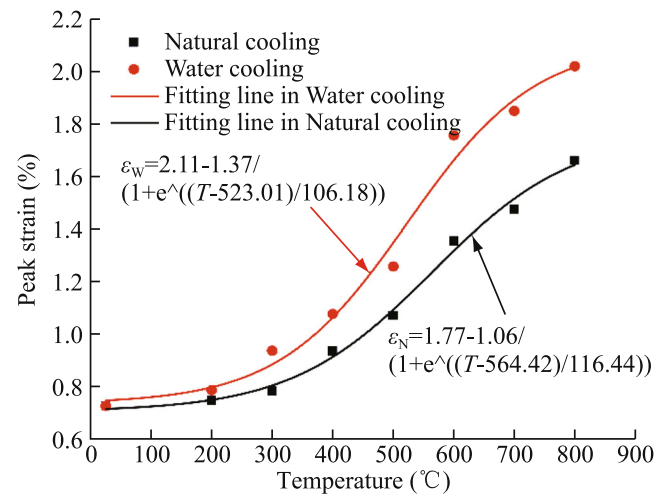


FIGURE 6 Variation of peak strain with the temperature under different cooling modes

peak strain increases with temperature, whereas the peak strain under water cooling is greater than that under natural cooling. This occurs mainly because there are many crack structures formed under the influence of thermal stress. The author wants to change to: The cracks constantly compact under the action of internal axial force, resulting in a large degree of rock deformation as the temperature increases. The fitting variance of the peak strain under natural cooling and water cooling is 0.99 and 0.98, respectively, and the fitting effect is improved. The specific formula is as follows:

$$\varepsilon_N = 1.77 - \frac{1.06}{1 + e^{\frac{T-564.42}{116.44}}}, \quad (1)$$

$$\varepsilon_W = 2.11 - \frac{1.37}{1 + e^{\frac{T-523.01}{106.18}}}, \quad (2)$$

where ε_N is the peak strain under natural cooling, ε_W is the peak strain under water cooling, and T is the testing temperature.

3.3 | Physical properties

The change of wave velocity can indicate the tightness of the rock's internal structure and can indirectly reflect the damage degree after heating at different temperatures (Deng et al., 2021). As is revealed, the wave velocity of the granite sample decreases with the increase in temperature (Figure 7), and the wave velocity under water cooling is lower than that of natural cooling. The change of wave velocity can be roughly divided into two stages. The first stage is from 25°C to 600°C, where the wave velocity decreases rapidly, and the internal structure is greatly damaged due to the phase transition of quartz, especially at 500–600°C. The second stage starts when the temperature exceeds 600°C, where the wave velocity decreases slowly, indicating that the thermal damage to granite has reached its limit at this time. It cannot significantly change the internal structure of the rock with increasing temperature.

Volume expansion and mass loss are the most direct manifestations of physical and chemical reactions that occur in rocks at high temperatures. Figure 8 shows that

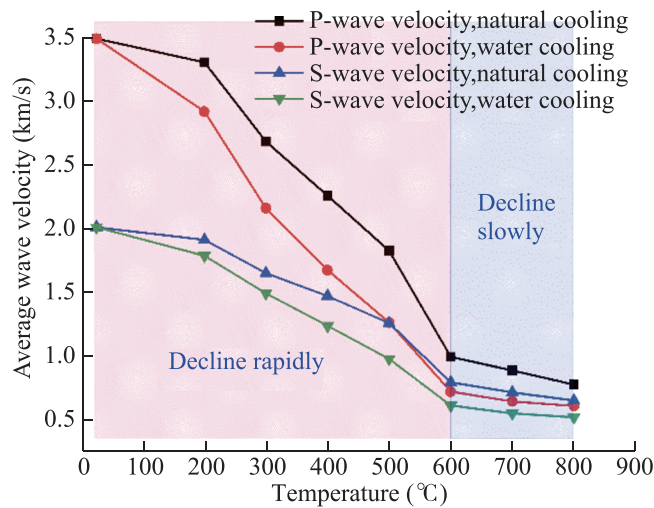


FIGURE 7 Variation of average wave velocity with temperature under different cooling modes

volume expansion and mass loss of granite increase as the temperature rises. The volume only displays a small increase below 400 °C, while the volume expansion rate begins to increase sharply when the temperature rises above 400 °C. The bulk expansion of quartz, albite, and other minerals under high temperatures equals the overall increasing volume of granite. Free water, crystal water, and structural water evaporate under a high-temperature environment, and some mineral components undergo chemical reactions, resulting in gas escape (W. Q. Zhang et al., 2016). All these factors lead to a continuous mass loss.

3.4 | Acoustic emission characteristics

The change of AE cumulative counts can be roughly divided into two stages: the calm stage and the rising stage (Figure 9). In the calm stage, the AE signal is a small energy event that is emitted stably. Results show that the accumulative counts increase to a small extent and the ringing counts are at a lower level. During the early period of the calm stage, the energy is in a state of aggregation and dissipation and a certain level of AE signals appear from the closure and compaction of the initial fracture. During the later period of the calm stage (i.e., the elastic stage), a steady and continuous AE phenomenon occurs. With the unstable development of rock expansion and micro-fracture, AE enters the rising stage. Specifically, the AE count is characterized by local increases and great leaps, and the cumulative AE count increases rapidly in a short time. AE events (R. Zhang et al., 2017) are transformed from low energy and small crack events in the early period to large events with high energy in the later period. The sample is completely destroyed and most of the energy is released; AE signals gradually decrease or even disappear. The released elastic energy is shown in the form of AE, whose performance is affected by temperature and cooling modes. At room temperature, the calm stage lasts for a long time, while the AE signal rises rapidly in a short time until the

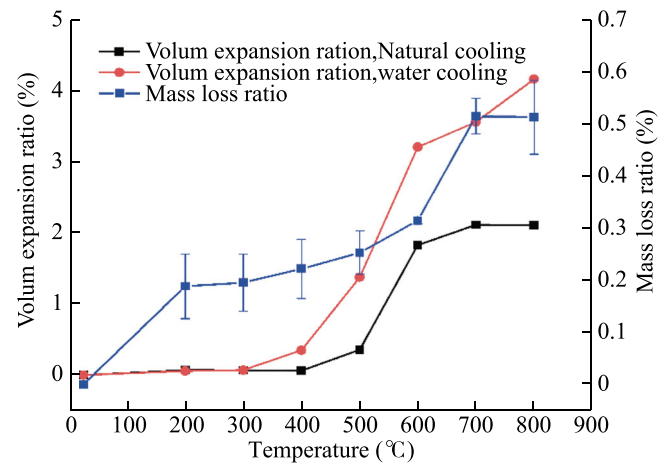


FIGURE 8 Variation of volume expansion ratio and mass loss ratio with temperature under different cooling modes

sample is destroyed. With the increase in temperature, the duration of the calm stage becomes shorter and can hardly be observed above 600 °C. An obvious AE signal appears at the beginning of loading, indicating that the granite undergoes significant damage above 600 °C. Under water cooling mode, the damage inside the rock is intensified and obvious AE signals could be observed at the initial loading stage at 500 °C. When the temperature rises above 600 °C, AE signals in the initial loading stage are maintained at a high level.

AE amplitude is the maximum amplitude value of the event signal waveform, which is directly related to the size of the event (R. Zhang et al., 2017). Figure 10 shows that low-amplitude events are the main distribution whereas high-amplitude events account for a small proportion. The number of AE amplitudes in each amplitude interval increases with the rise of temperature. Among them, the number of AE amplitudes at 200 °C ranging from 40 to 50 dB is lower than that at 25 °C, indicating that the number of fracture events at 200 °C is lower than that at 25 °C. This further explains that the mechanical properties of granite are enhanced to a certain extent at 200 °C. The distribution characteristics of the AE amplitude under water cooling are similar to those under natural cooling. However, the number of AE amplitudes in each interval is higher than that under natural cooling. Moreover, Figure 10b reveals that the AE amplitude of granite at 800 °C is lower than 700 °C, suggesting that there are fewer failure events at 800 °C. This can also explain why UCS is a little higher than that at 700 °C. During the test, it was also found that the low amplitude was mainly distributed in the initial loading stage. Meanwhile, the high amplitude was mainly distributed when the specimen was damaged. The change of AE amplitude can also be used as an early-warning signal to against the destruction of rocks.

AE parameters include ringing counts, events, energy, and hits (R. Zhang et al., 2017). Figure 11 shows that the sum of AE counts, AE events, and AE hits increase with the rise of temperature. The AE parameters of rapid cooling in water are generally higher than those of natural cooling. This indicates that the internal structure

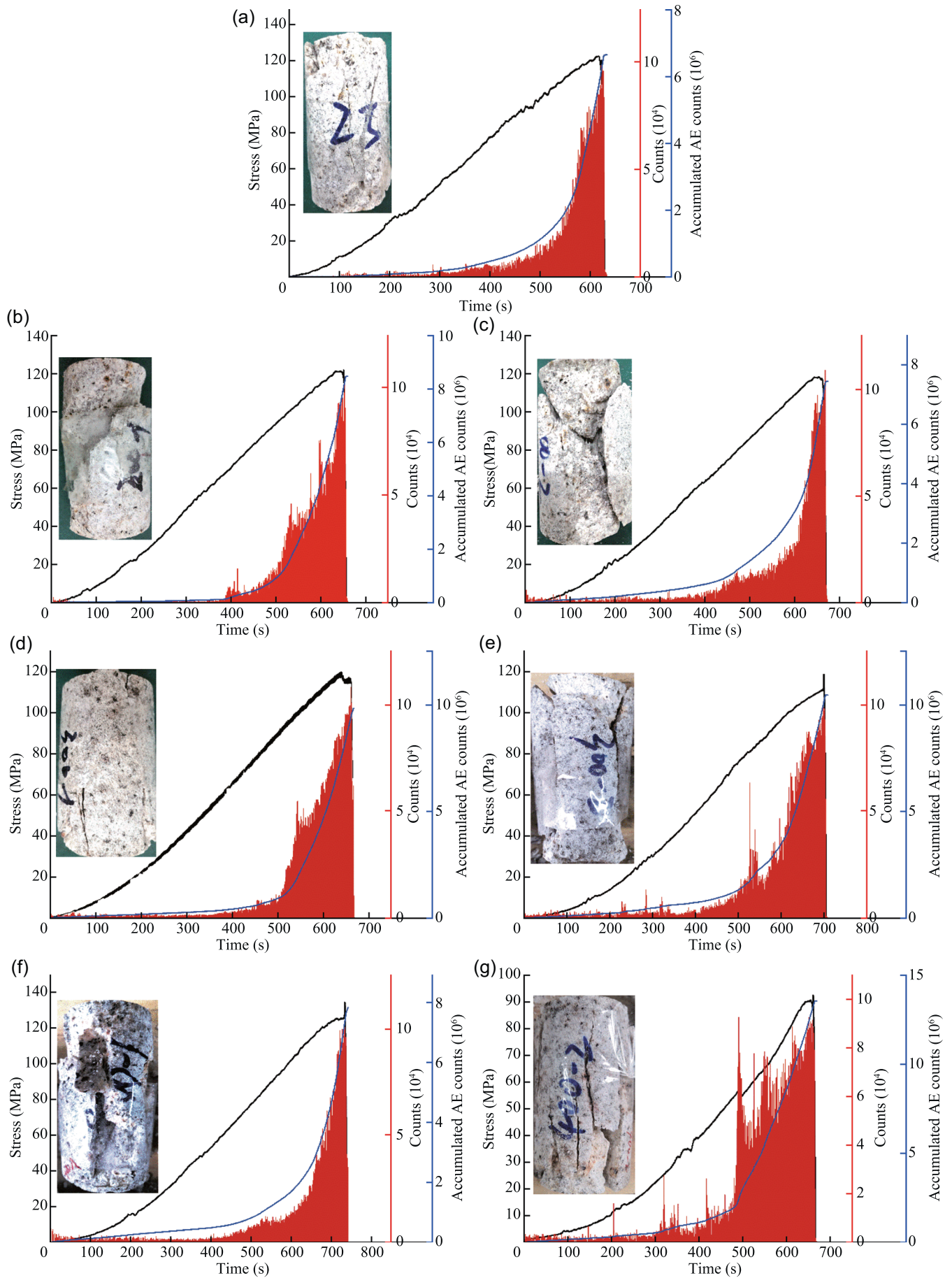


FIGURE 9 Characteristics of AE in the whole loading process and failure pattern under different temperatures in natural cooling and water cooling: (a) AE characteristics at room temperature; (b) AE characteristics at 200 °C after natural cooling; (c) AE characteristics at 200 °C after water cooling; (d) AE characteristics at 300 °C after natural cooling; (e) AE characteristics at 300 °C after water cooling; (f) AE characteristics at 400 °C after natural cooling; (g) AE characteristics at 400 °C after water cooling; (h) AE characteristics at 500 °C after natural cooling; (i) AE characteristics at 500 °C after water cooling; (j) AE characteristics at 600 °C after natural cooling; (k) AE characteristics at 600 °C after water cooling; (l) AE characteristics at 700 °C after natural cooling; (m) AE characteristics at 700 °C after water cooling; (n) AE characteristics at 800 °C after natural cooling; (o) AE characteristics at 800 °C after water cooling

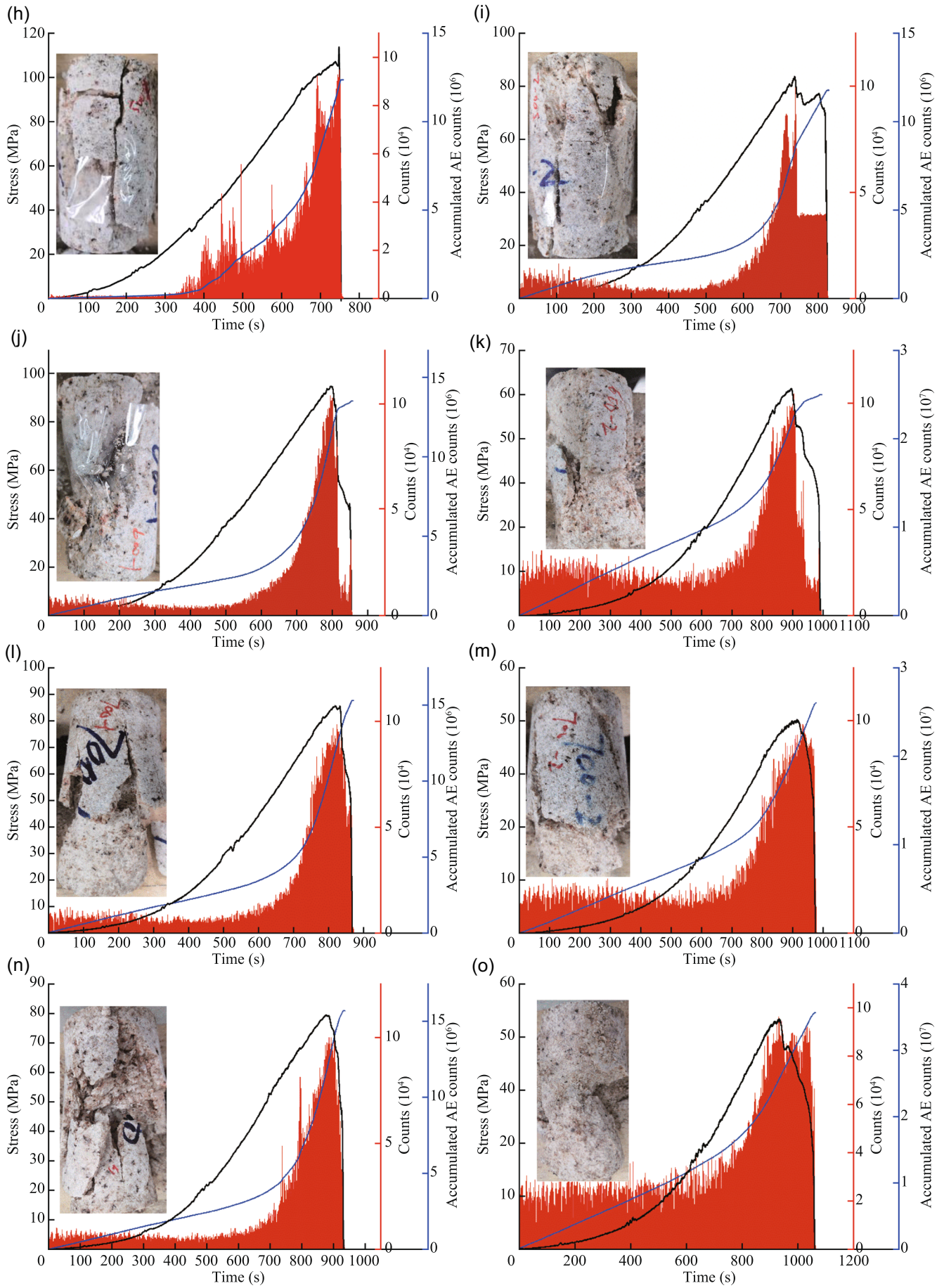


FIGURE 9 (Continued)

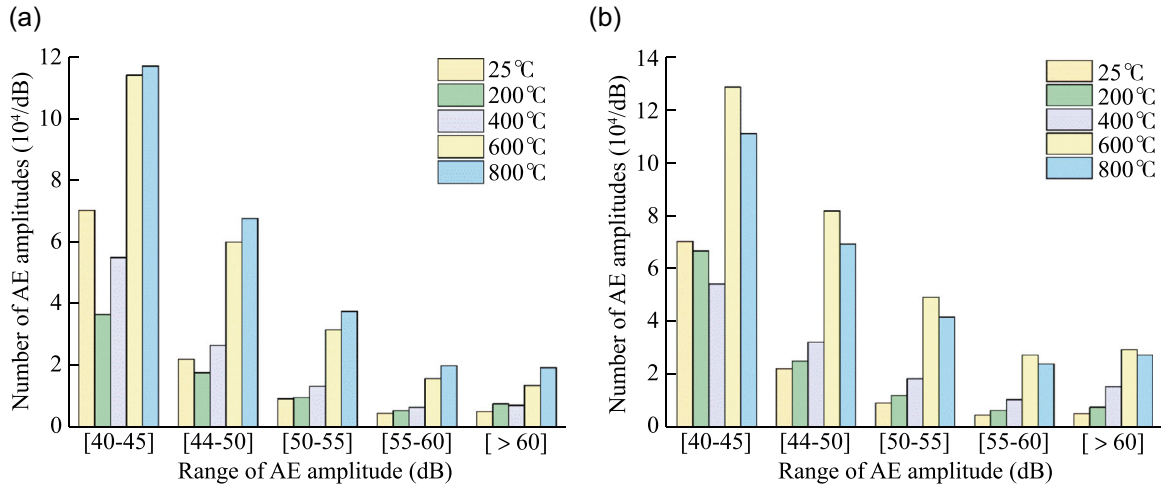


FIGURE 10 The distribution characteristics of AE amplitudes under different temperatures in different cooling modes: (a) natural cooling; (b) water cooling

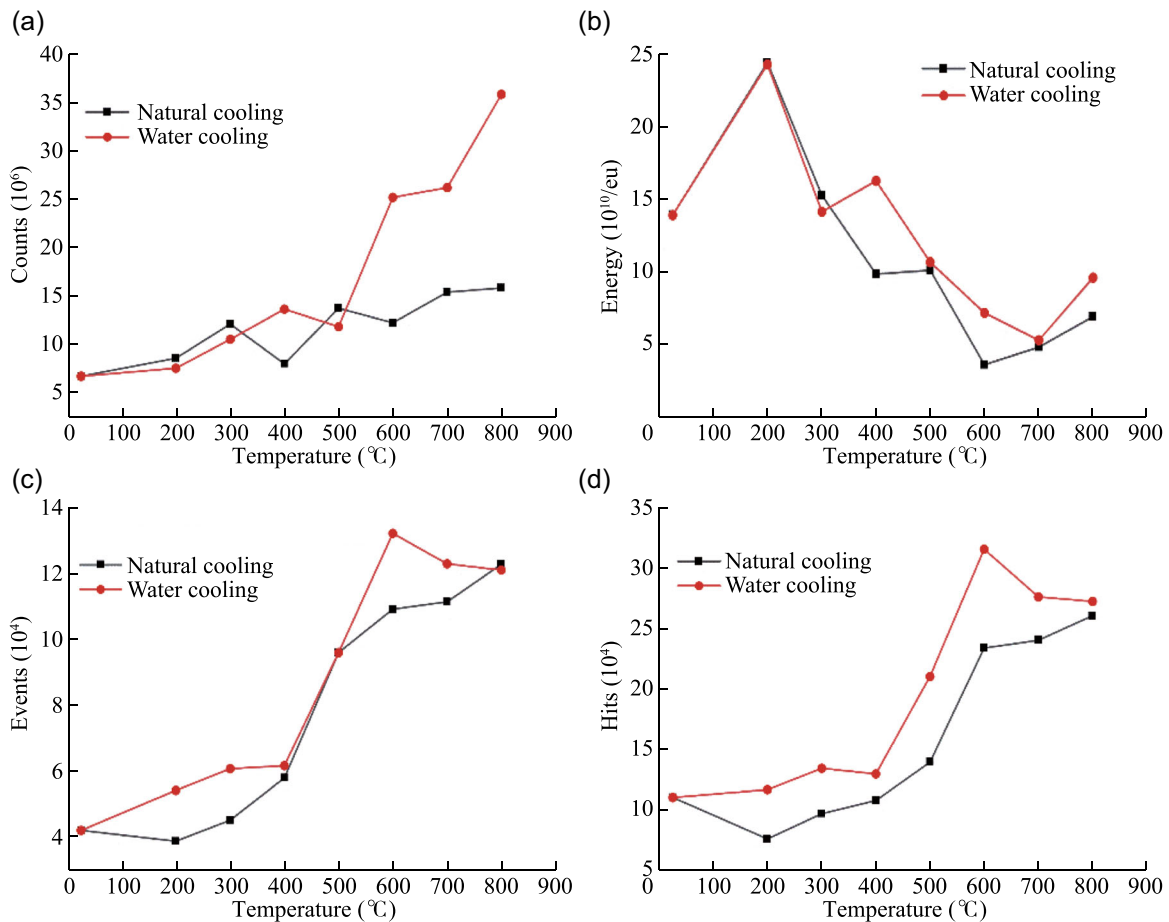


FIGURE 11 The change of the sum of AE parameters with temperature under both cooling modes: (a) Counts; (b) energy; (c) events; (d) hits

of the granite is significantly weakened after water cooling. Figure 11b shows that AE energy generally decreases with the rise of temperature, which may be related to the transition from brittleness to ductility. There is still a certain amount of energy without consumption after the rock is destroyed in the ductile state.

The time-varying b -value can effectively reflect the changing state of the internal fracture at different loading stages (R. Zhang et al., 2017). The calculation formula of AE b -value is as follows (Fu et al., 2016):

$$\lg N = a - b \frac{A_{dB}}{20}, \quad (3)$$

where A_{dB} is the AE amplitude, which is usually set by itself according to the data situation. N is an equal number of AE events with amplitudes $> A_{dB}$, and is selected in a specific time window to determine the b -value; a is a constant, and b is the parameter needed to obtain. A scanning algorithm was adopted to conduct the calculation. In total, 4000 events were taken as a fixed

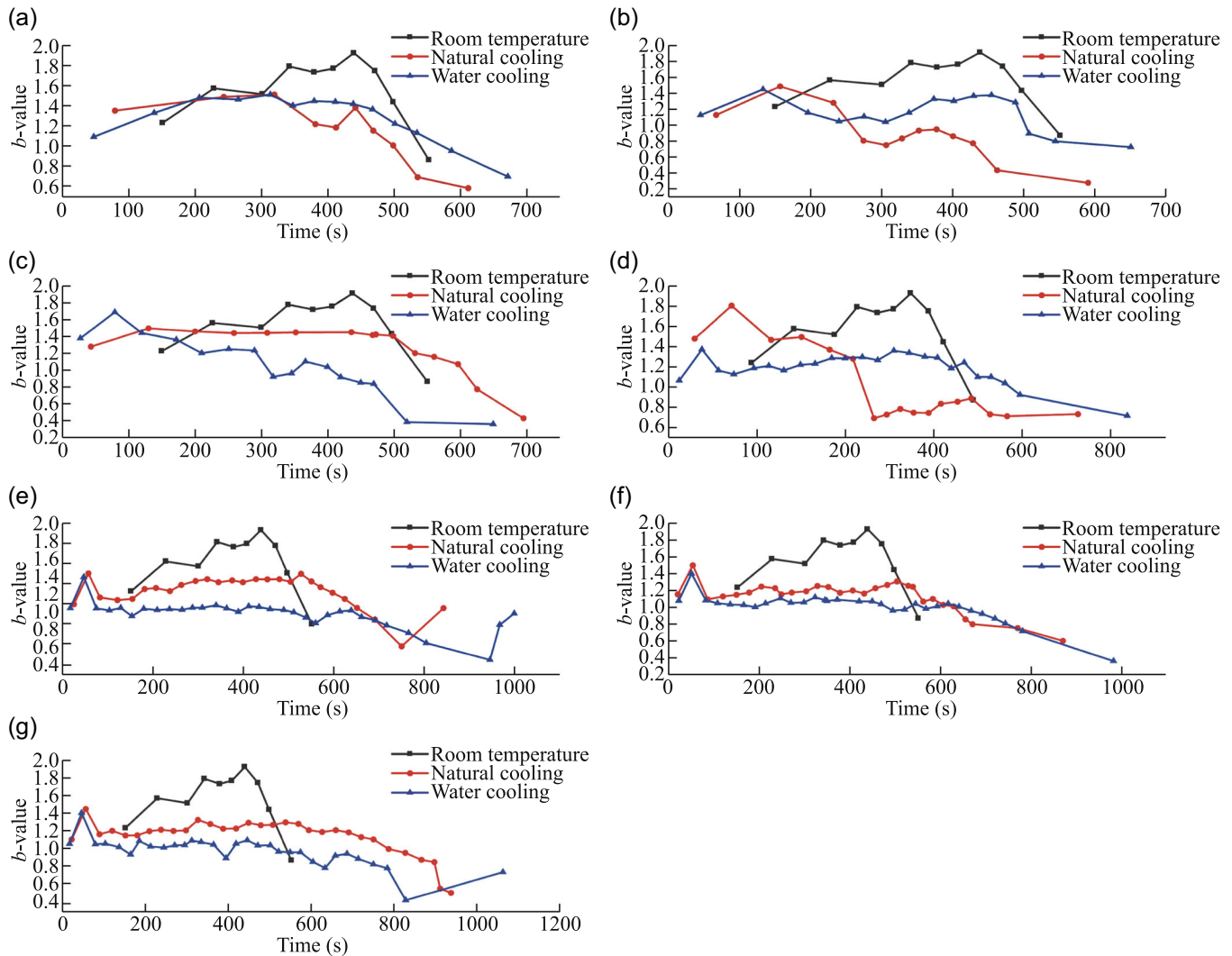


FIGURE 12 Variation of AE b -value with time under different temperatures in water cooling and natural cooling modes

time window for calculating the b -values based on AE data to ensure the feasibility of calculation.

The cooling method has a great impact on the b -value, which is presented as a dynamic development, as seen in Figure 12. At the beginning of loading, the AE b -value displays small fluctuations, reflecting that the micro-cracks are slowly changed. The proportion of AE events of different sizes remains unchanged, and the crack state of different scales is relatively constant, representing gradual progress of stable expansion. The AE b -value begins to rise as the load increases, indicating that the proportion of small-scale micro-cracks begins to enlarge accordingly. When the stress reaches a certain level, the AE b -value decreases rapidly, and the internal cracks of the granite exhibit an unstable growth state. A decrease in the b -value was reported during the failure of rock samples subjected to uniaxial compressive loading (Hirata et al., 1987; Main et al., 1989). Figure 12 roughly shows that the b -value of granite at room temperature is generally higher than that at other temperatures. Further, the AE b -value of granite under natural cooling is higher than that under water cooling. This indicates that the destruction of granite at room temperature involves small-scale events, whereas it is mainly destroyed by large-scale events when it is cooled by water.

The variation of AE characteristics can be further explained by the final failure mode of granite. Figure 9 demonstrates that a larger size of lumpiness after failure at room temperature is produced in granite. With the increase in experimental temperature, there are more small-scale fragments of granite under the action of compressive stress; many powders even appear when the temperature rises above 600 °C. Accordingly, it can be concluded that the failure mode of granite is more complex under the water-cooling mode. This indicates that the number and connectivity of cracks formed in the granite are positively related with the rise of temperature. Further, the difference in the cooling rate within the granite leads to greater thermal stress, which further promotes the expansion and penetration of micro-cracks.

4 | DISCUSSION

According to the variation of UCS in Figure 5, the mechanical properties are influenced by heating and cooling modes. Meanwhile, the different AE characteristics in Figure 9 show that the physical and mechanical properties of samples change under a high-temperature environment. The essence of these changes is the shift in the

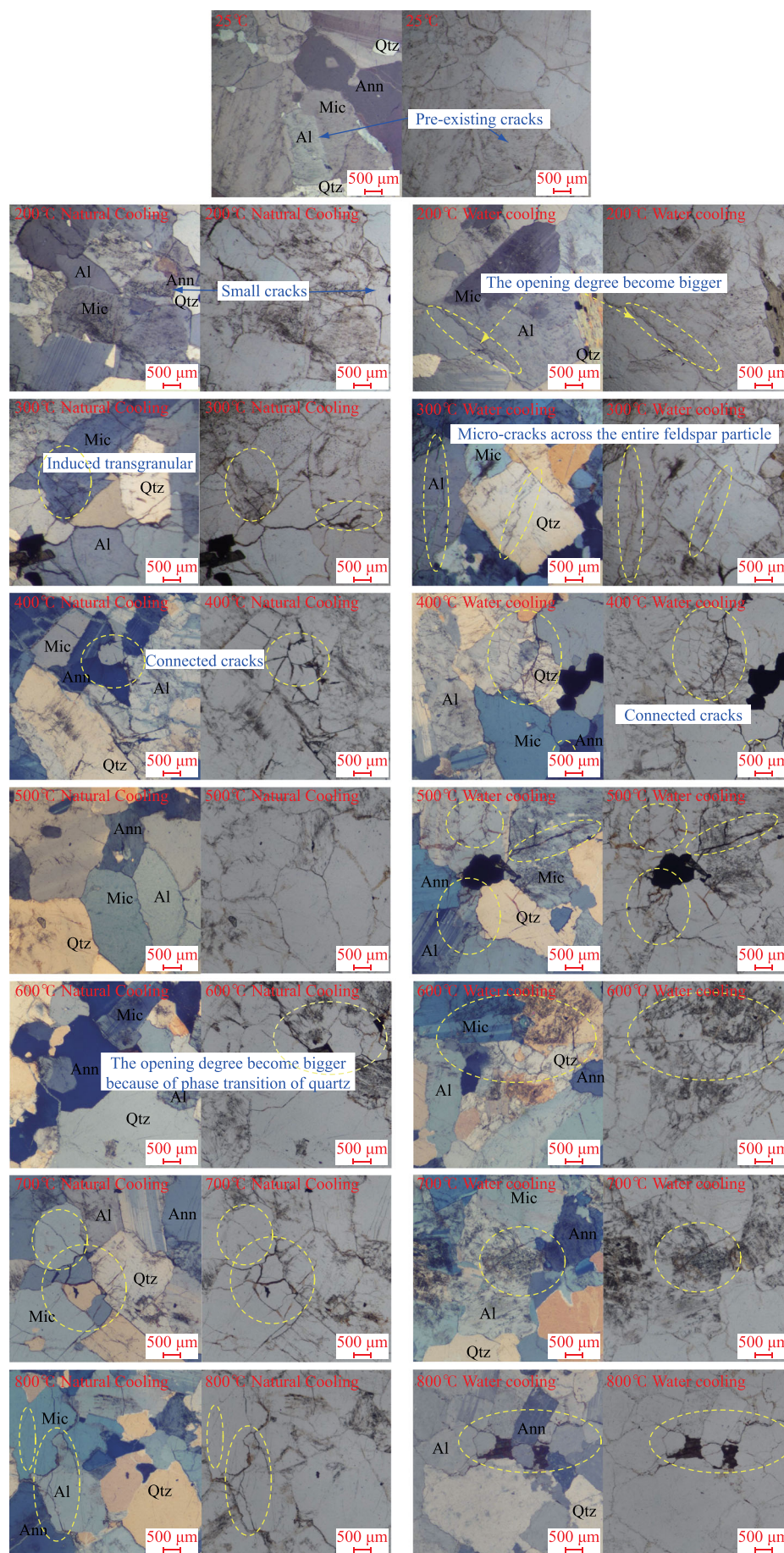


FIGURE 13 The microscopic image of grain after thermal treatment under both cooling modes (the yellow circles represent the opening and connectivity of the micro-cracks)

internal structure. Therefore, it is necessary to further explore the influence of heating and cooling modes on the internal structure. Figure 13 shows the internal structure of granite under a polarized light microscope when the granite sample is heated at different temperatures. At 25 °C, there are no obvious cracks in the quartz, albite, mica, and other mineral particles of granite, and the binding among these mineral particles is relatively close. By comparing the micro-images of single slices and orthogonal modes, the opening degree among different mineral particles like quartz, albite, mica, and the same mineral particles becomes larger with the rise of testing temperatures. This is mainly due to the difference in the thermal expansion coefficient, which leads to uncoordinated deformation among mineral particles. There are also many micro-cracks in the mineral crystal, which are called trans-granular cracks caused by the thermal stress exceeding the limited strength of the mineral crystal. Notably, as the temperature rises, the micro-cracks continuously nucleate, expand, and penetrate, finally forming a crack network.

Great changes in the number, shape, and connectivity of cracks are generated due to the different cooling rates of high-temperature granite. In the case of water cooling, the stress distribution of mineral particles is significantly different due to the large difference in cooling rates inside and outside the sample. Thermal stress of different directions and sizes is generated in the same mineral particle, and the cracking of the whole mineral particle is produced due to the extremely uneven stress distribution. Thus, micro-cracks of different scales and sizes are produced, and these mineral particles are more likely to fall off under the impact of flowing water. In summary, the stress under water-cooling mode varies greatly, which justifies the granite's weakened mechanical properties.

The change in the physical and mechanical properties of rocks is caused by the evolution of micro-cracks. The greater the number of micro-cracks is, the greater the damage degree of granite will be. According to the research results of Kim et al. (2020) there is a certain relation between crack density and acoustic parameters. The longitudinal wave velocity and dynamic elastic modulus can be used to estimate the crack density. The specific formula involved is as follows:

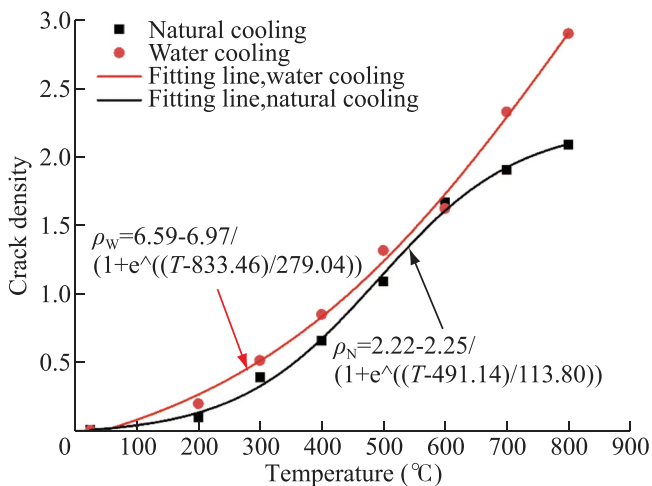


FIGURE 14 The variation of crack density with temperature

$$E^* = \rho_m V_P^2 \frac{(1 + \mu^*)(1 - 2\mu^*)}{1 - \mu^*}, \tag{4}$$

$$\mu^* = \frac{\left(\frac{V_P}{V_S}\right)^2 - 2}{2 \left(\frac{V_P}{V_S}\right)^2 - 1}, \tag{5}$$

$$E \cong E^*, \tag{6}$$

$$\mu \cong \mu^*, \tag{7}$$

$$\rho = \frac{1}{h} \left[(1 + \mu) \frac{E_0}{E} - (1 + 3\mu_0) \right], \tag{8}$$

$$h = 16 \left(1 - \mu_0^2 \right) / 9 \left(1 - \frac{\mu_0}{2} \right), \tag{9}$$

where, ρ is crack density; h is the geometric factor; μ is the overall Poisson's ratio; E is the elastic modulus; μ^* is dynamic Poisson's ratio; E^* is the dynamic elastic modulus; V_P is the P-wave velocity; V_S is shear wave velocity; ρ_m is the density of the rock.

The crack density of rocks heated at different temperatures can be calculated by Formula 8. Figure 14 shows the relation between the calculated crack density and temperature. As is suggested, the crack density increases with the rise of temperature; in contrast, the crack density formed under rapid water cooling is higher than that under natural cooling. This illustrates the physical and mechanical properties of granite and the evolution of AE characteristics. By fitting the variation of crack density, it can be found that the crack density conforms to a certain functional relation with temperature:

$$\rho_N = 2.22 - \frac{2.25}{1 + e^{\frac{T-491.14}{113.80}}} \quad R^2 = 0.99, \tag{10}$$

$$\rho_W = 6.59 - \frac{6.97}{1 + e^{\frac{T-833.46}{279.04}}} \quad R^2 = 0.99, \tag{11}$$

where, ρ_W is the crack density under water cooling; ρ_N is the crack density under natural cooling; T is the

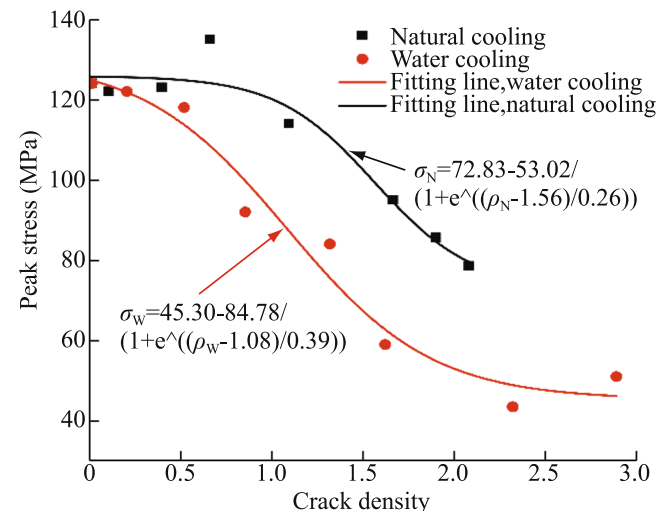


FIGURE 15 The variation of peak stress with crack density

temperature. Figure 15 shows that the peak stress of granite decreases gradually with the increase of crack density. The peak stress of granite decreases rapidly under the water cooling at the same crack density. There is a certain relation between the peak stress of the rock and the crack density. The fitting equation is expressed as follows:

$$\sigma_N = 72.83 - \frac{53.02}{1 + e^{\frac{\rho_N - 1.56}{0.26}}} \quad R^2 = 0.91, \quad (12)$$

$$\sigma_W = 45.30 - \frac{84.78}{1 + e^{\frac{\rho_W - 1.08}{0.39}}} \quad R^2 = 0.95, \quad (13)$$

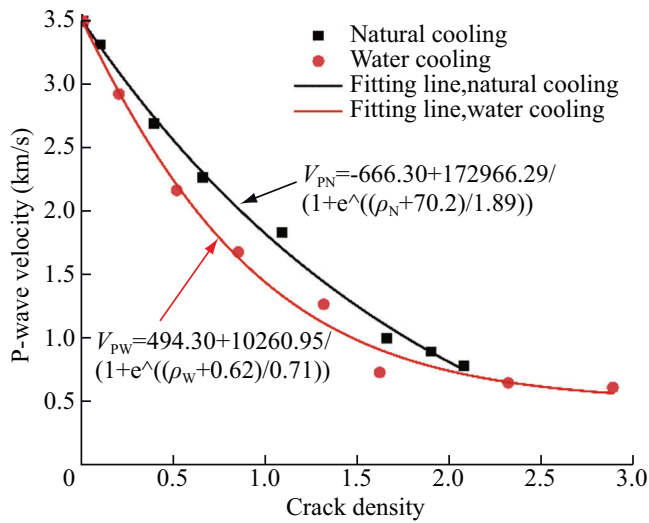


FIGURE 16 The variation of P-wave velocities with crack density

where, σ_N is the peak stress during natural cooling and σ_W is the peak stress when cooled by water.

The existence of the crack leads to a significant change in the longitudinal wave velocity of rocks (Figure 7). Figure 16 shows the relation between the longitudinal wave velocity and crack density. In general, the longitudinal wave velocity decreases with the increase of crack density. More specifically, the number of micro-cracks formed in the granite under the water cooling causes the longitudinal wave velocity to decrease faster. This further explains the variation of longitudinal wave velocity in granite. By fitting the relation between the longitudinal wave velocity and the crack density, it can be concluded that:

$$V_{PN} = -666.30 + \frac{172966.29}{1 + e^{\frac{\rho_N + 70.2}{1.89}}} \quad R^2 = 0.99, \quad (14)$$

$$V_{PW} = 494.30 + \frac{10260.95}{1 + e^{\frac{\rho_W + 0.62}{0.71}}} \quad R^2 = 0.98, \quad (15)$$

where, V_{PW} is the longitudinal wave velocity under water cooling and V_{PN} is the longitudinal wave velocity under natural cooling.

The stress-strain response characteristics and AE characteristics of rocks are also significantly different due to the essential reason for altered mineral structure. Figure 17 shows the mineral composition pattern of granite at different temperatures. The main minerals of granite at room temperature include quartz, albite, microcline, and annite. No obvious changes are found in mineral types, content, and diffraction angle at different temperatures. This indicates that granite's mineral composition is relatively stable and does not weaken the physical and mechanical properties within

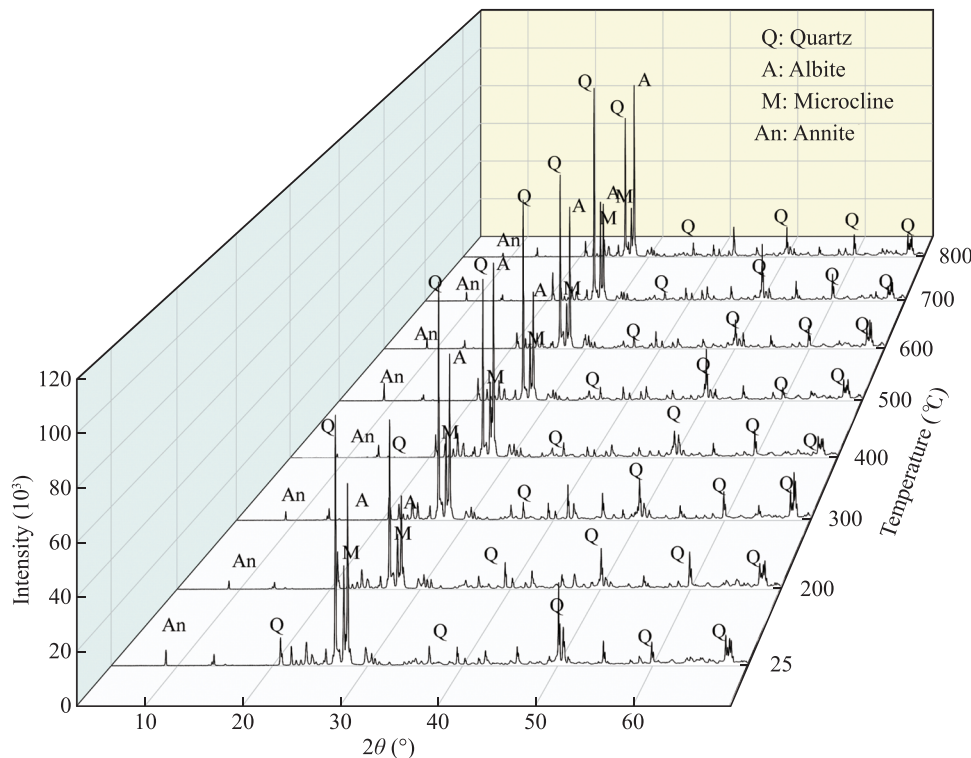


FIGURE 17 XRD patterns of granite at different temperatures

the temperature range. However, high temperature has a weak influence on the degree of mineral deformation at different cooling rates. The thermal conductivity of quartz is higher than annite and feldspar, which leads to different degrees of thermal expansion between quartz and the other minerals. The higher the temperature is, the greater the uncoordinated deformation will be. Additionally, some minerals undergo phase transitions at high temperatures, which seriously affects the mechanical properties of granite. For example, quartz undergoes a phase transition at 573 °C, and its volume expands to a great extent.

5 | CONCLUSIONS

This paper mainly studies the physical and mechanical properties of granite when the sample is heated at 25–800 °C and then treated by water cooling and natural cooling. It reveals the damage mechanism of high-temperature granite under different cooling rates. The main conclusions are as follows:

- (1) When the granite is heated at high temperatures, its physical and mechanical properties change greatly. The higher the cooling rate is, the more drastic changes in granite properties appear. On the whole, the peak stress decreases with the rise of temperature. Specifically, the peak stress of naturally cooled granite increases to a certain extent due to the crack closure at 25–400 °C. The peak strain of granite under water cooling is higher than that under natural cooling and increases as the temperature rises. The longitudinal wave velocities and shear wave velocities decrease significantly when the granite sample is cooled by water. When the granite sample is cooled by water, the expansion degree of granite is significantly higher than that of natural cooling.
- (2) The AE *b*-value under water cooling is generally lower than that under natural cooling, which means that large-scale crack development is the main factor in water cooling and the damage degree is greater. At the same time, according to the AE count, AE event, AE energy, distribution of AE amplitude, it can be seen that the AE signal is more active when the granite sample is cooled by water than when it is naturally cooled. Further, the AE activity signal tends to be stronger with the rise of temperature.
- (3) The damage mechanism of high-temperature granite under different cooling rates was analyzed by polarizing microscope and XRD. The cooling rate mainly affects the degree of uncoordinated deformation of minerals. Meanwhile, the influencing mechanism of temperature is related to the type and content of minerals. Quartz has high thermal conductivity and a phase transition occurs at 573 °C, which seriously affects the physical and mechanical properties of granite. Granite minerals are relatively stable within the temperature range of the test. The crack development was further verified according to the formula derived from acoustic parameters. The results reveal that the crack density

of high-temperature granite is larger when it is cooled by water, and the density increases with the rise of temperature.

ACKNOWLEDGMENTS

This study is supported by the financial support from the National Natural Science Foundation of China (41702326), the Innovative Experts, Long-term Program of Jiangxi Province (jxsq2018106049), the Natural Science Foundation of Jiangxi Province (20202ACB214006), and the Supported by Program of Qingjiang Excellent Young Talents, Jiangxi University of Science and Technology.

CONFLICT OF INTEREST

The authors declare no conflict of interest.

DATA AVAILABILITY STATEMENT

The original contributions presented in the study are included in the article/Supplementary Material; further inquiries can be directed to the corresponding author.

ETHICS STATEMENT

Ethics statement consent for publication not applicable.

REFERENCES

- Avanthim I, Gamage RP. An influence of thermally-induced micro-cracking under cooling treatments: mechanical characteristics of Australian granite. *Energies*. 2018;11(6):1-24. <https://www.mdpi.com/1996-1073/11/6/1338>
- Cai C, Li G, Huang Z, Shen Z, Tian S, Wei J. Experimental study of the effect of liquid nitrogen cooling on rock pore structure. *J Nat Gas Sci Eng*. 2014;21:507-517.
- Cai CZ, Gao F, Huang ZW, Hou P. Evaluation of coal damage and cracking characteristics due to liquid nitrogen cooling on the basis of the energy evolution laws. *J Nat Gas Sci Eng*. 2016;29:30-36. [doi:10.1016/j.jngse.2015.12.041](https://doi.org/10.1016/j.jngse.2015.12.041)
- Cai CZ, Huang Z, Li GS, Gao F, Wei JW, Li R. Feasibility of reservoir fracturing stimulation with liquid nitrogen jet. *J Petrol Sci Eng*. 2016;144:59-65. [doi:10.1016/j.petrol.2016.02.033](https://doi.org/10.1016/j.petrol.2016.02.033)
- Cai CZ, Li GS, Huang ZW, Tian SC, Shen ZH, Fu X. Experiment of coal damage due to super-cooling with liquid nitrogen. *J Nat Gas Sci Eng*. 2015;22:42-48. [doi:10.1016/j.jngse.2014.11.016](https://doi.org/10.1016/j.jngse.2014.11.016)
- Cha M, Alqohtani NB, Yin X, Kneafsey T, Yao BW, Wu YS. Laboratory system for studying cryogenic thermal rock fracturing for well stimulation. *J Petrol Sci Eng*. 2017;156:780-789. [doi:10.1016/j.petrol.2017.06.062](https://doi.org/10.1016/j.petrol.2017.06.062)
- Chaki S, Takarli M, Agbodjan W. Influence of thermal damage on physical properties of a granite rock: porosity, permeability and ultrasonic wave evolutions. *Constr Build Mater*. 2008;22:1456-1461.
- Chen S, Yang CH, Wang GB. Evolution of thermal damage and permeability of Beishan granite. *Appl Therm Eng*. 2017;110:1533-1542. [doi:10.1016/j.applthermaleng.2016.09.075](https://doi.org/10.1016/j.applthermaleng.2016.09.075)
- Chen Y, Wang C. Thermally induced acoustic emission in westerly granite. *Geophys Res Lett*. 1980;7(7):1089-1092. [doi:10.1029/GL007i012p01089](https://doi.org/10.1029/GL007i012p01089)
- Chen YF, Hu SH, Wei K, Hu R, Zhou CB, Jing LR. Experimental characterization and micromechanical modeling of damage-induced permeability variation in Beishan granite. *Int J Rock Mech Min Sci*. 2014;71:64-76. [doi:10.1016/j.ijrmms.2014.07.002](https://doi.org/10.1016/j.ijrmms.2014.07.002)
- Datt P, Kapil JC, Kumar A. Acoustic emission characteristics and *b*-value estimate in relation to waveform analysis for damage response of snow. *Cold Reg Sci Technol*. 2015;119:170-182. [doi:10.1016/j.coldregions.2015.08.005](https://doi.org/10.1016/j.coldregions.2015.08.005)
- Deng LC, Li XZ, Wu Y, et al. Study on mechanical damage characteristics of granite with different cooling methods. *J China Coal Soc*. 2021;46(S1):187-199. [doi:10.13225/j.cnki.jccs.2020.1284](https://doi.org/10.13225/j.cnki.jccs.2020.1284)

- Fairhurst C, Hudson J. Draft ISRM suggested method for the complete stress-strain curve for intact rock in uniaxial compression. *Int J Rock Mech Min Sci.* 1999;36(3):279-289.
- Fu B, Zhao ZH, Wang HQ, Wang YX. Precursor information study on acoustic emission characteristics of marble under uniaxial cyclic loading-unloading. *J China Coal Soc.* 2016;41(8):1946-1953. doi:10.13225/j.cnki.jccs.2016.0345
- Ge ZL, Sun Q. Acoustic emission (AE) characteristics of granite after heating and cooling cycles. *Eng Fract Mech.* 2018;200:418-429. doi:10.1016/j.engfracmech.2018.08.001
- Gens A, Guimaraes LN, Garcia-Molina A, Alonso EE. Factors controlling rock-clay buffer interaction in a radioactive waste repository. *Eng Geol.* 2002;64:297-308. doi:10.1016/S0013-7952(02)00026-1
- Gomez-Heras M, Gomez-Villalba LS, Fort R. Cambios de fase en litoarenitas calcareas con la temperatura: implicaciones para el deterioro causado por incendios. *Mala Rev Soc Esp Mineral.* 2010;135:101-102.
- Han GS, Jin HW, Su HJ, Yi Q, Wu JY, Gao Y. Experimental research on mechanical behaviors of water-cooled sandstone after high temperature treatment. *J Univer Mining Technol.* 2020;49(1):69-75. doi:10.13247/j.cnki.jcumt.001101
- Hirata T, Satoh T, Ito K. Fractal structure of spatial distribution of micro-fracturing in rock, geophys. *J R Astron Soc.* 1987;90:369-374. doi:10.1111/j.1365-246X.1987.tb00732.x
- Jin PH, Hu YQJ, Shao JX, Liu ZJ, Hu YF. Study on pore structure and permeability of granite subjected to heating and water quenching. *J Taiyuan Univer Technol.* 2019;50(4):478-484. doi:10.16355/j.cnki.issn1007-9432tyut.2019.04.011
- Johnson B, Gangi AF, Handin J. Thermal cracking of rock subjected to slow, uniform temperature changes. *Int J Rock Mech Min Sci Geomech Abstr.* 1979;16(2):23. doi:10.1016/0148-9062(79)91483-9
- Kim BC, Chen J, Kim JY. Relation between crack density and acoustic nonlinearity in thermally damaged sandstone. *Int J Rock Mech Min Sci.* 2020;125:1041-1071. doi:10.1016/j.ijrmms.2019.104171
- Li C, Hu YQ, Zhang CW, et al. Brazilian split characteristics and mechanical properties evolution of granite after cyclic cooling at different temperatures. *Chin J Rock Mech Eng.* 2020;39:1-11. doi:10.13722/j.cnki.jrme.2020.0247
- Liu S, Xu J. Mechanical properties of Qinling biotite granite after high temperature treatment. *Int J Rock Mech Mining Sci.* 2014;71:188-193. doi:10.1016/j.ijrmms.2014.07.008
- Liu S, Xu J. An experimental study on the physico-mechanical properties of two post-high-temperature rocks. *Eng Geol.* 2015;185(4):63-70. doi:10.1016/j.enggeo.2014.11.013
- Main IG, Meredith G, Jones C. A reinterpretation of the precursory seismic b-value anomaly from mechanics. *Geophys J Int.* 1989;96:131-138. doi:10.1016/0148-9062(89)92948-3
- Murru A, Freire, Lista DM, et al. Evaluation of post-thermal shock effects in Carrara Marble and Santa Caterina di Pittinuri limestone. *Constr Build Mater.* 2018;186:1200-1211. doi:10.1016/j.conbuildmat.2018.08.034
- Nara Y, Morimoto K, Yoneda T. Effects of humidity and temperature on subcritical crack growth in sandstone. *Int J Solids Struct.* 2011;48:1130-1140. doi:10.1016/j.ijsolstr.2010.12.019
- Shao ZL, Wang Y, Tang XH. The influences of heating and uniaxial loading on granite subjected to liquid nitrogen cooling. *Eng Geol.* 2020;271:1056-1014. doi:10.1016/j.enggeo.2020.105614
- Souley M, Homand F, Pepa S, Hoxha D. Damage-induced permeability changes in granite: a case example at the URL in Canada. *Int J Rock Mech Min Sci.* 2001;28(2):297-310. doi:10.1016/S1365-1609(01)00002-8
- Sun H, Sun Q, Deng WN, Zhang WQ, Lv C. Temperature effect on microstructure and P-wave propagation in Linyi sandstone. *Appl Therm Eng.* 2017;115:913-922. doi:10.1016/j.applthermaleng.2017.01.026
- Urquhart A, Bauer S. Experimental determination of single-crystal halite thermal conductivity, diffusivity and specific heat from -75°C to 300°C. *Int J Rock Mech Mining Sci.* 2015;78:350-352. doi:10.1016/j.ijrmms.2015.04.007
- Vazquez P, Shushakova V, Gomez-Heras M. Influence of mineralogy on granite decay induced by temperature increase: experimental observation and stress stimulation. *Eng Geol.* 2018;189:58-67. doi:10.1016/j.enggeo.2015.01.026
- Wang P, Xu JY, Liu S, Chen TF. Research of dynamic mechanical properties of sandstone at high temperature. *Acta Armamentarii.* 2013;34(2):203-208.
- Wang ZW, Liu QS, Wang YX. Thermo-mechanical FDEM model for thermal cracking of rock and granular materials. *Powder Technol.* 2021;393:807-823. doi:10.1016/j.powtec.2021.08.030
- Wu SC, Guo P, Zhang SH. Study on thermal damage of granite based on Brazilian splitting test. *Chin J Rock Mech Eng.* 2018;37:3805-3815. doi:10.13722/j.cnki.jrme.2018.0576
- Wu XG, Huang ZG, Li R, et al. Investigation on the damage of high-temperature shale subjected to liquid nitrogen cooling. *J Nat Gas Sci Eng.* 2018;57:284-294. doi:10.1016/j.jngse.2018.07.005
- Wu Y, Li XZ, Huang Z, Wang YC, Deng LC. Effect of thermal damage on tensile strength and microstructure of granite: a case study of Beishan, China. *Geomech Geophys Geo-Energy Geo-Resour.* 2021;7:82. doi:10.1007/s40948-021-00278-x
- Xi BP, Wu YC, Zhao YS, Wang L, Zhang BP, Niu XM. Experimental investigations of compressive strength and thermal damage capacity characterization of granite under different cooling modes. *Chin J Rock Mech Eng.* 2020;39(2):286-300. doi:10.13722/j.cnki.jrme.2019.0782
- Zhang F, Konietzky H, Fruhwirt T, Li YW, Dai YJ. Impact of cooling on fracturing process of granite after high-speed heating. *Int J Rock Mech Min Sci.* 2020;125:1041-1055. doi:10.1016/j.ijrmms.2019.104155
- Zhang F, Zhang YH, Yu YD, Hu DW, Shao JF. Influence of cooling rate on thermal degradation of physical and mechanical properties of granite. *Int J Rock Mech Min Sci.* 2020;129:1042-1085. doi:10.1016/j.ijrmms.2020.104285
- Zhang R, Ai T, Gao MZ. *Basic Theory and Experimental Study of Acoustic Emission in Rocks.* Sichuan University Press; 2017.
- Zhang W, Sun Q, Hao SQ, Geng JS, Lv C. Experimental study on the variation of physical and mechanical of rock after high temperature treatment. *Appl Therm Eng.* 2016;98:1297-1304. doi:10.1016/j.applthermaleng.2016.01.010
- Zhang WQ, Lv C. Effects of mineral content on limestone properties with exposure to different temperatures. *J Petrol Sci Eng.* 2020;188:1069-1041. doi:10.1016/j.petrol.2020.106941
- Zhang WQ, Sun Q, Hao SQ, Geng JS, Lv C. Experimental study on the variation of physical and mechanical properties of rock after high temperature treatment. *Appl Therm Eng.* 2016;98:1297-1304. doi:10.1016/j.applthermaleng.2016.01.010

AUTHOR BIOGRAPHIES



Xiaozhao Li is a professor at the China University of Mining and Technology, Xuzhou, China. His main research field is fine exploration, collaborative development, and disaster prevention in underground space. He is the director of the State Key Laboratory of Deep Geotechnics and Underground Engineering, Underground Space Research Center, Nanjing University, and Nanjing Strategic Emerging Industries Innovation Center. In addition, he is the chair of ACUUS-GEO, and a member of the evaluation expert group of the National Natural Science Foundation of China, National Key Research and Development Program, and National Science and Technology Cooperation Special Project, and so forth.

Dr. Yun Wu is a lecturer at China University of Mining and Technology, Xuzhou, China. He is a member of the Chinese Society of Rock Mechanics and Engineering. His main research interests cover

nuclear waste disposal, underground energy storage and deep geothermal exploitation. Until now, Dr. Wu has been awarded the Jiangsu excellent post-doctoral support program and participated in some national major engineering projects. He has published more than 10 peer-reviewed papers.

How to cite this article: Deng LC, Li XZ, Wu Y, et al. Influence of cooling speed on the physical and mechanical properties of granite in geothermal-related engineering. *Deep Underground Sci and Eng.* 2022;1:40-57. doi:10.1002/dug2.12011